

VARIABLE RATE SPRAYER SYSTEM

Largim Zhuta, Katharine Ott, Manoj Sharma* and Christopher Kitts.

Santa Clara University, Santa Clara, CA

ABSTRACT

Precision spraying is a technique that relies on a precisely targeted metered delivery of a desired fluid. It utilizes sensors and automation to optimize the application of chemicals. By adjusting the application rate in real-time based on specific crop needs variable rate sprayers minimize chemical use, reduce environmental impact, and increase crop yield. In this paper, we present a sprayer system for our in-house modular rover that can administer fluid in a controlled manner. It offers discrete left and right independent spray control, each within the range of 120-400 L/h. Tests conducted in the field show the performance within 0.1-4.8 % of the commanded value. Furthermore, we lay out the framework for a high-level sprayer-rover interface controller to intelligently adapt and command the desired flow rates.

Keywords: Precision spraying, Variable flow rate, Prescription fluid administration

1. INTRODUCTION

The advent of robotics and automation in the field of agriculture helps in the emergence of novel techniques which were previously impossible due to technical limitations and high cost. Among others, precision spraying is one such domain that is adopting technology to improve efficiency and emphasize sustainable practices. Current research in the area of automated sprayer systems includes automated vision-based weed detection and targeted spraying [6–8]. These techniques have also been implemented in a large production field showcasing the viability of precision spraying [9]. Other notable work in the field of variable rate precision sprayer shows the benefit of a model based sprayer control an efficient means of chemical administration [10–13]. One Smart Spray [2] from Bosch is a precision sprayer system that leverages high-resolution cameras to detect weeds in real time and spray herbicide only where needed, reducing the use and cost of inputs for growers.

In terms of type of spray vehicle, there are three broad categories namely, network of fluid lines laid in ground, aerial vehicle [14], and self-propelled vehicle system. The work presented here is a type of self-propelled system which is designed as a modular subsystem to an existing rover system, referred to as Agbot [15] developed in the Robotic Systems Lab. The motivation in designing this sprayer system was to add on to the functionality of the Agbot, which is designed in-house [15] at Santa Clara University. This is one of the modular tools designed to integrate with the Agbot, or other similar robotic platform [16], where the rover acts as a support system for the sprayer module. Multiple pre-existing systems were examined and are broken down into performance factors in Table 1.

1.1 Ethical Implications

Agriculture is one of the areas where robots have started to show their potential in various field operations [17, 18]. Labor-intensive work profiles and challenging work conditions may be addressed through robotic devices and potential co-exist during the transition phase [19], thereby allowing laborers to be reallocated to higher skilled work. Furthermore, the agriculture industry itself faces a dramatic shortage of labor, leading to high labor costs and unharvested crops [20, 21]. Robotic and automation technology can also be used to expand the use of precision agriculture practices in order to lead to more efficient, cost-effective and sustainable farming practices [22].

Whilst this sprayer design was created with the greater good in mind, we acknowledge that it poses some ethical issues. Like most things, automating the agriculture spraying process has both positive and negative impacts. Some positive aspects include decreasing health risk to farmers when spraying chemicals, decreasing the amount of heavy labor farmers have to perform, and specified input control on how much is spraying each section, minimizing waste. Some negative impacts include possible displacement of labor, reduction of farmer's autonomy, and a potential increase of damaging impacts of agricultural runoff by increasing production.

*Corresponding author: mk.sharma@ieee.org

Documentation for asmecnf.cls: Version 1.37, August 23, 2024.

TABLE 1: Analysis of pre-existing sprayer systems.

Manufacturer	Performance	Leading Feature	Limitation	Cite
See & Spray, John Deere	Spray while moving at a speed of up to 19 km/h.	Cameras and Machine Learning based precision weed targeting.	No dual-product solution system or split tank.	[1]
One Smart Spray, Bosch	Up to 95% application accuracy.	Weed targeting. Green on green & green on brown performance. LED lighting to spray night and day.	Limited to corn, soy, cotton, sunflower and canola.	[2]
Bilberry, Trimble	Reduces herbicide usage by 90%. Up to 25 km/h rover speed.	Weed targeting Green on green & green on brown performance.	Green on green & limited to certain weeds and Grass.	[3, 4]
Greeneye Technology	Reduces herbicide usage by 90%. Up to 25 km/h rover speed.	Weed targeting, classifies weeds by species.	Green on green & green on brown performance.	[5]

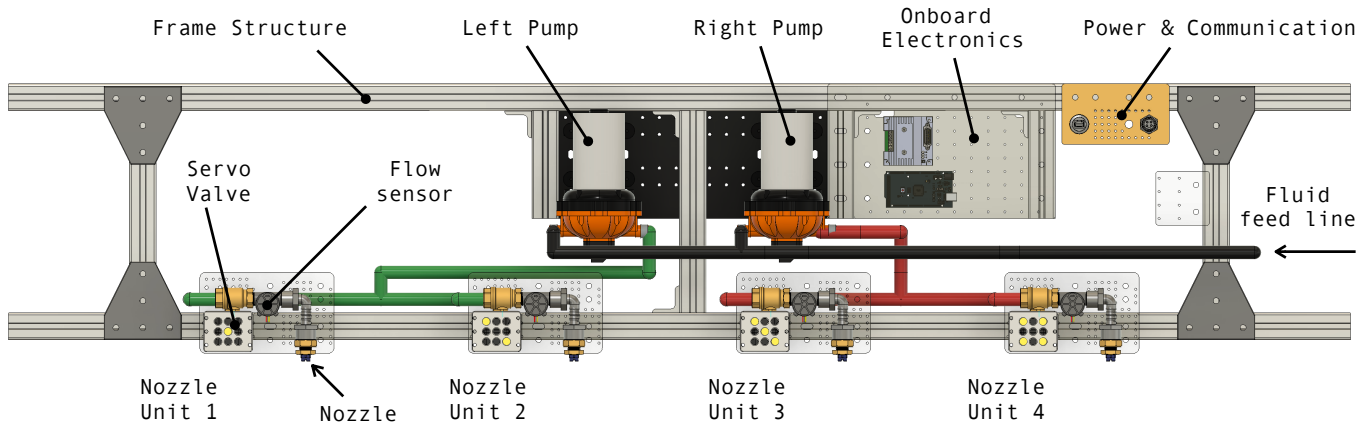


FIGURE 1: SPRAYER SYSTEM OVERVIEW.

1.2 Contributions

1. Modular sprayer system for the rover,
2. Test and validate the spray performance, and
3. Create a foundation for a prescription based spray controller.

2. DESIGN PHASE

During the early developmental phase we considered a sprayer system with eight nozzles spread equidistantly to cover a furrow width of approximately 1.5 meters. A single pump was chosen as the main actuator to move the fluid. Each nozzle receives the fluid from the common pump outlet with a solenoid-plunger valve in series respectively. The valves can be commanded to a fully open or fully close position to control the flow rate by modifying the width of each pulse. During the testing phase we discovered that the highly discrete nature due to the low valve-fidelity results in a spray pattern where there are large gaps of no-spray zone. Additionally, the pump of choice is a positive displacement pump which means the pump power directly relates to the flow rate. This results in a highly coupled system where flow rate of each nozzle affects one another.

Based on the lesson learnt from the previous work, we have redesigned the system with key improvement to meet the design

requirement. The new design is explained in the subsequent sections. The system overview is split into four different subsections. The first three subsections provide an overview of the mechanical, electrical and software architecture of the sprayer module followed by a description on the specifics of how the sprayer module is integrated within the rover system in mechanical, electrical and software sense.

2.1 Mechanical Sub-system

The mechanical sub-system consists of two systems: the frame-structure and the plumbing. The frame structure serves as the backbone of the sprayer system. It is assembled from aluminum T-slotted rails. All of the subsystems are mounted onto the frame structure. The plumbing sub-system includes (1) fluid reservoir, (2) positive-displacement pumps, silicone vacuum seal tubing, and (4) modular Nozzle Units (NUs) as shown in Fig. 1 and Fig. 2. The NUs are composed of (3) key components: a servo valve, a flow sensor, and a nozzle. NU 1, NU 2, and the left pump constitute the *left bank* of the sprayer system. NU 3, NU 4, and the right pump make up the *right bank*. Each bank operates independently of the other: they only share the same reservoir tank.

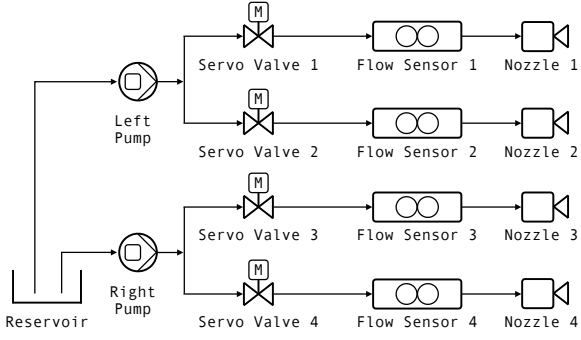


FIGURE 2: SPRAYER SYSTEM FLUID CIRCUIT DIAGRAM.

2.2 Electrical Sub-system

The key electrical subsystem comprises the pump, servo controlled valve, and flow rate sensor. The two pumps are controlled by a dual-channel (RoboteQ) motor controller. An Arduino Mega 2560 is the microcontroller of choice which controls the respective pump power, servo-valve, and receives the instantaneous flow rate information from all four nozzle units. An onboard computer (Jetson Nano) is dedicated to allow the information exchange between the sprayer and the rover system. The entire sprayer system is designed to operate at 12 VDC which is provided by the rover.

2.3 Software Sub-system

Three functional systems exist within the software subsystem: data acquisition, data display, and the controller. Real-time flow rate data and pump power is recorded for each flow sensor and each pump. It is stored in the Robot Operating System (ROS) bag data type. The aforementioned real-time data is displayed in a serial monitor within the Arduino IDE. A closed loop Proportional-Integral (PI) controller with a feed-forward term is implemented for the sprayer system. The source code for the sprayer system is maintained on *Github* at https://github.com/irahulone/sys_sprayer.

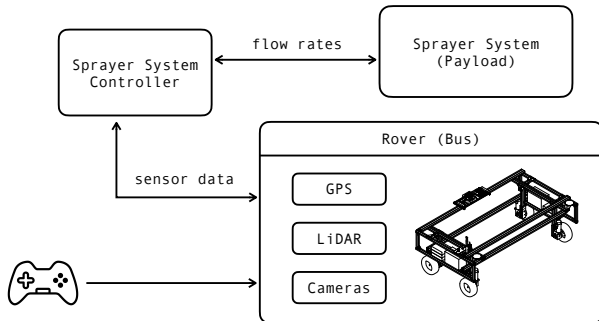


FIGURE 3: SPRAYER AND ROVER SYSTEM INTEGRATION.

2.4 Sprayer-Rover Integration

In a *bus* and *payload* analogy, the sprayer system is the payload which relies on the rover (*the bus*) to receive the necessary support needed for the mission. The T-slot aluminium extrusion based construction allows for a convenient mechanical integration

using off-the-shelf brackets. The sprayer and rover system, both, uses *ROS* as the main control framework [15] which streamlines the flow of data among various subsystems. Fig. 3 shows sprayer-rover integration. The sprayer controller has access to the position sensors, speed, vision system and other onboard data to compute desired flow rate information.

3. CONTROL AND VALIDATION

This section focuses on the feedback control design to achieve a desired flow rate followed by a series of field tests to validate the performance of the system in the field environment.

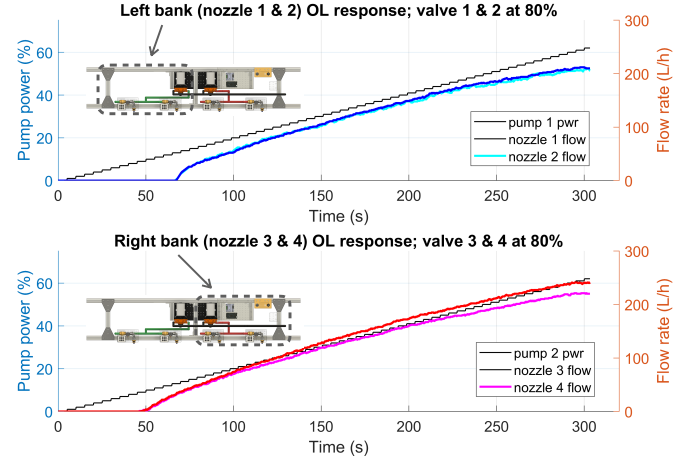


FIGURE 4: SPRAYER SYSTEM OPEN-LOOP NOZZLE FLOW RATE LEFT AND RIGHT BANK TIME VARYING RESPONSE TO A RAMP INPUT; VALVES AT 80%.

3.1 Control System Design

The reference inputs (or setpoints) to the system are the desired flow rates for the left and right bank, \bar{q}_l and \bar{q}_r , respectively. Separate and unique mapping functions are used to convert the desired flow rates into left and right pump powers, \hat{p}_l and \hat{p}_r , for each bank, shown in Fig. 5. The mapping function M maps the pump power \hat{p} to the actual flow rate q , with M_l and M_r depicting left and right bank, respectively.

$$M_l : \hat{p}_l \mapsto q_l, \text{ and} \quad (1)$$

$$M_r : \hat{p}_r \mapsto q_r. \quad (2)$$

The maps are empirically determined by experimentation as shown in Fig. 4. The desired flow rate signals are then summed with the measured flow rates, creating resultant error signals for the two banks. The error signal is then fed into a Proportional-Integral controller shown in Fig. 5. The output of the left and right bank controllers yield a pump power value. The pumps then produce a flow rate, which is fed through the servo valves, flow sensor, and nozzle; this ultimately outputs the measured flow rate. The left and right pump powers are

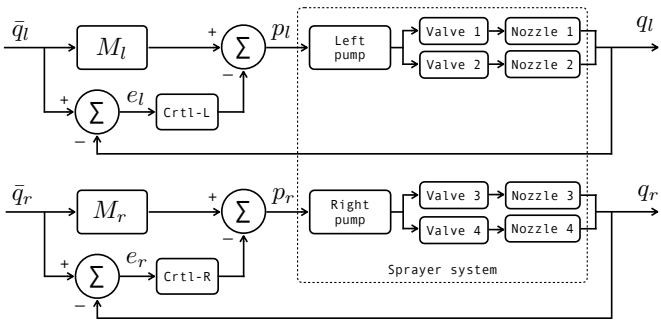


FIGURE 5: BLOCK DIAGRAM REPRESENTATION OF SPRAYER CONTROL SYSTEM.

$$u_l = p_l = M_l^{-1} \bar{q}_l + (k_{p_l} e_l + k_{i_l} \int e_l), \text{ and} \quad (3)$$

$$u_r = p_r = M_r^{-1} \bar{q}_r + (k_{p_r} e_r + k_{i_r} \int e_r). \quad (4)$$

where,

$$e_l = \bar{q}_l - q_l, \text{ and} \quad (5)$$

$$e_r = \bar{q}_r - q_r. \quad (6)$$

3.2 Testing and Results

The sprayer is a closed loop system, delivering a desired flow rate using a closed-loop controller. The performance of the system is highly dependent on the accuracy of each flow sensor. System performance verification was performed concurrently with system performance testing. The testing occurred on a nearby farm in an environment that would likely resemble the rover and sprayer system's natural area of operation: one with external factors such as wind, dust, and uneven, rocky terrain, as shown in Fig. 6. The testing occurred while the rover was in motion at a speed within the range of 0.1 m/s to 0.4 m/s.

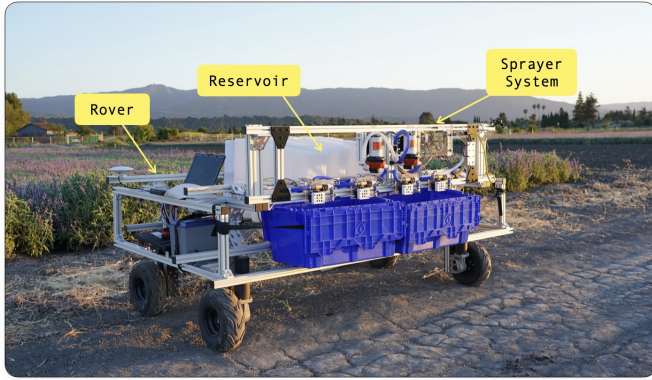


FIGURE 6: SPRAYER SYSTEM WITH ROVER IN A TEST FIELD.

In Fig. 7, the desired flow is set to 131 L/h for both left and right banks. It takes the left and right bank approximately 8.5 s to settle within a 15% error band. The reason behind the larger

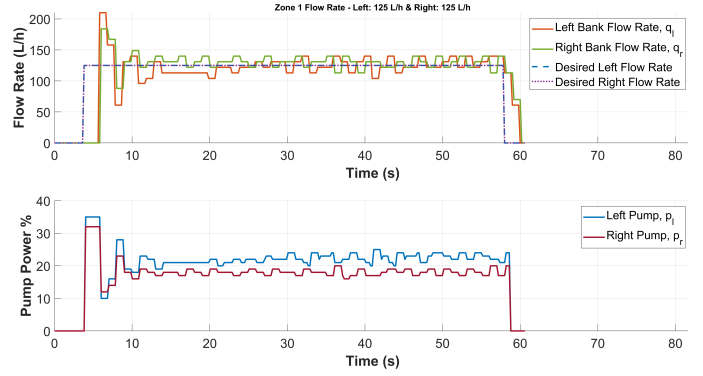


FIGURE 7: TOP PLOT SHOWS THE LEFT AND RIGHT BANK FLOW RATE TRANSIENT RESPONSE TO A STEP DESIRED FLOW RATE INPUT OF 131 L/h FOR BOTH LEFT AND RIGHT BANK. BOTTOM PLOT SHOWS PUMP POWERS COMPUTED BY THE CLOSED-LOOP CONTROLLER.

error band is because the system never fully settles below a 15% error. This is likely due to limitations in the sensor's resolution and computation. The recorded flow rate data appears to take on discrete values. In the steady state region of Fig. 7, the recorded data takes on one of the following values: 113 L/h, 122 L/h, 131 L/h, and 140 L/h. This indicates that the resolution of the sensor is roughly 9 L/h per bit. Given this finding, performing root mean squared (RMS) calculations on the entirety of data provides greater insight over the steady state behavior. The RMS value for the left bank in Fig. 7 is 125.3 L/h, and the RMS value for the right bank is 130.8 L/h. The RMS value is compared against the desired flow rate of 131 L/h for both banks; it equates to an error of 4.8% and 0.1% for the left and right bank, respectively. The verification portion involved collecting the dispensed water via collection bins and noting the total time elapsed during the trial. Average flow rates for each bank were then calculated by dividing the total volume of water collected in the bins by the total time of the trial. Note that this method of verification is prone to human error in measurement and reaction time, resolution error in the analog measuring tools, evaporation due to wind, etc. From the verification test, the calculated flow rates are determined to be 133.4 L/h and 131.7 L/h for the left and right banks, respectively. This amounts to an error of 1.8% and 0.5% between the desired flow rates and averaged flow rates of the system.

Further system performance testing is carried out for different desired flow rates as shown in Fig. 8 and Fig. 9. In Fig. 8, the settling time for the system is shorter, and the error band is smaller; for a 10% error band, the settling time is approximately 2.5 s for both banks. The RMS values are 353.4 L/h and 211.0 L/h for the left and the right bank, respectively. It equates to errors of 1.8% and -0.4%. For the verification test performed in Fig. 8, the desired flow rates are 360 L/h and 210 L/h, respectively. The average flow rates are calculated to be 356.0 L/h and 211.8 L/h for the left and right bank respectively: yielding errors of 1.1% and 0.8%. Furthermore, in Fig. 9, a similar result can be seen when the desired flow rates for the left and right banks are swapped with the other. The settling time for 10% error band

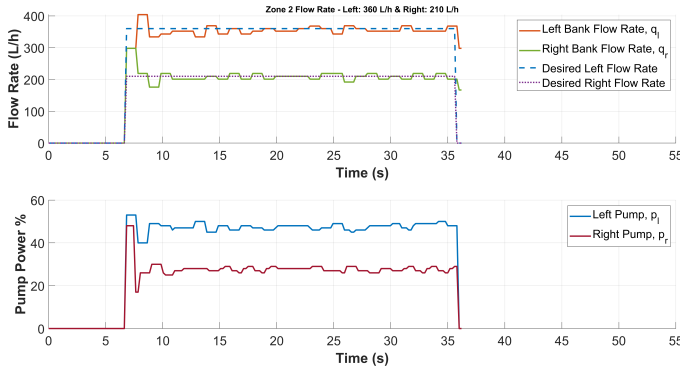


FIGURE 8: TOP PLOT SHOWS THE LEFT AND RIGHT BANK FLOW RATE RESPONSE TO A STEP DESIRED FLOW RATE INPUT OF 360 L/h FOR THE LEFT BANK AND 210 L/h FOR THE RIGHT BANK. BOTTOM PLOT SHOWS PUMP POWERS COMPUTED BY THE CLOSED-LOOP CONTROLLER.

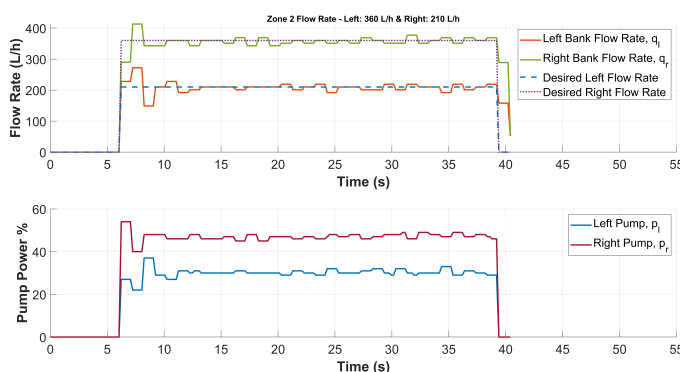


FIGURE 9: TOP PLOT SHOWS THE LEFT AND RIGHT BANK FLOW RATE RESPONSE TO A STEP DESIRED FLOW RATE INPUT OF 210 L/h FOR THE LEFT BANK AND 360 L/h FOR THE RIGHT BANK. BOTTOM PLOT SHOWS PUMP POWERS COMPUTED BY THE CLOSED-LOOP CONTROLLER.

is also approximately 2.5 s for both banks. The RMS values are 208.0 L/h and 353.4 L/h for the left and right bank, respectively. This yields errors of 0.9% for the left bank and 1.8% for the right bank.

In Fig. 9 the desired flow rates for the left and right bank are 210 L/h and 360 L/h, respectively. The average flow rates for the left and right bank were 217.5 L/h and 352.3 L/h, amounting to errors of 3.6% and 2.1%. The results from the system performance tests indicate that the system is able to administer the desired flow rate within a 4.8% RMS error margin. (i.e. RMS flow sensor reading compared to the desired flow rate). The system performance verification shows that the administered flow rate is accurate to within a 3.6% error margin (i.e. the physical amount of water collected over a finite time compared to the desired flow rate).

Figure 10 and Table 2 shows a performance test for a multi-zone trial. Five arbitrary zones were created, each with different desired flow rates. The multi-zone trial was performed while the rover was moving at a constant speeds of 0.3 m/s. The zones were advanced via button toggling through the rover joystick

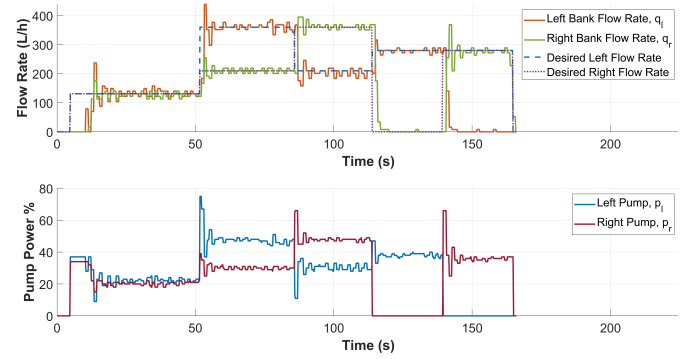


FIGURE 10: MULTI-ZONE TIME RESPONSE.

TABLE 2: Zone-level flow rates (L/h).

Zone	Left-bank flow			Right-bank flow		
	Des.	Sen.	Act.	Des.	Sen.	Act.
1	131.0	125.3	133.4	131.0	130.8	131.7
2	360.0	353.4	356.0	210.0	211.0	211.8
3	210.0	208.0	217.5	360.0	353.4	352.3

controller; this displays the potential ability to control the spray parameters externally; in other words, the rover may be able to control the spray parameters based on global positioning system (GPS) data, light detection and ranging (LiDAR), or vision data as shown in Fig. 3. GPS and mapping technologies could ensure that chemicals are applied only where needed, reducing waste and improving crop health. The performance of the multi-zone run is consistent with what was seen in the step-input responses. The settling time between zone transitions is between 2 to 3 s. One notable exception can be seen in the plot during the initial power up; the reason behind the larger than expected settling time of the first zone is due to the pumps needing time to prime the system. Left at rest for a sufficient amount of time, the water drains downward and out of pumps, thus causing a larger initial settling time.

4. CONCLUSION

We have designed and constructed a modular sprayer attachment for the existing Agbot Rover which provides the necessary infrastructure for the mission. The closed-loop controller of the sprayer has been shown to be capable of administering the desired flow rate within an error margin between 0.1% and 4.8%. Lastly, a framework has been created between the sprayer and rover which will allow for the exchange of information between the two. The main purpose of the framework is to develop a prescription-based controller.

ACKNOWLEDGMENTS

We thank Jagos Jovanovic, Jordan Hibbs, Ian Watts, and all other members who have assisted with performing experiments and who have contributed to the development of the sprayer & rover system. We also thank Larry Jacobs and Martial Cottle park members in San Jose who have generously allowed us to run experiments.

REFERENCES

- [1] Deer, John. "See and Spray Technology." (2024). Accessed 2024, URL <https://www.deere.com/en/sprayers/see-spray/>.
- [2] Blakely, Bob. "One Smart Spray." (2023). Accessed 2024, URL <https://www.businesswire.com/news/home/20230912991567/en/>.
- [3] Bilberry. "Bilberry." (2024). Accessed 2024, URL <https://bilberry.io/applications/#benefits>.
- [4] Bilberry. "Bilberry." (2024). Accessed 2024, URL <https://bilberry.io/faq/>.
- [5] Technology, Greeneye. "Greeneye Technology." (2024). Accessed 2024, URL <https://greeneye.ag/technology/>.
- [6] Guan, Yangang, Chen, Dexin, He, Ketai, Liu, Ying and Li, Li. "Review on research and application of variable rate spray in agriculture." *2015 IEEE 10th Conference on Industrial Electronics and Applications (ICIEA)*: pp. 1575–1580. 2015. DOI [10.1109/ICIEA.2015.7334360](https://doi.org/10.1109/ICIEA.2015.7334360).
- [7] Berenstein, Ron and Edan, Yael. "Automatic Adjustable Spraying Device for Site-Specific Agricultural Application." *IEEE Transactions on Automation Science and Engineering* Vol. 15 No. 2 (2018): pp. 641–650. DOI [10.1109/TASE.2017.2656143](https://doi.org/10.1109/TASE.2017.2656143).
- [8] Aravind, R, Daman, M and Kariyappa, B S. "Design and development of automatic weed detection and smart herbicide sprayer robot." *2015 IEEE Recent Advances in Intelligent Computational Systems (RAICS)*: pp. 257–261. 2015. DOI [10.1109/RAICS.2015.7488424](https://doi.org/10.1109/RAICS.2015.7488424).
- [9] do Nascimento, Gustavo Henrique, Weber, Felipe, Almeida, Gabrielle, Terra, Fábio and Drews, Paulo Lilles Jorge. "A Perception System for an Autonomous Pesticide Boom Sprayer." *2019 Latin American Robotics Symposium (LARS), 2019 Brazilian Symposium on Robotics (SBR) and 2019 Workshop on Robotics in Education (WRE)*: pp. 86–91. 2019. DOI [10.1109/LARS-SBR-WRE48964.2019.00023](https://doi.org/10.1109/LARS-SBR-WRE48964.2019.00023).
- [10] Felizardo, Kleber R., Mercaldi, Heitor V., Oliveira, Vilma A. and Cruvinel, Paulo E. "Modeling and Predictive Control of a Variable-Rate Spraying System." *2013 8th EUROSIM Congress on Modelling and Simulation*: pp. 202–207. 2013. DOI [10.1109/EUROSIM.2013.46](https://doi.org/10.1109/EUROSIM.2013.46).
- [11] Zhang, Zhihong, Zhu, Heping, Salcedo, Ramón and Wei, Zhiming. "Assessment of Premixing In-Line Injection System Attached to Variable-Rate Orchard Sprayer." *Pesticide Formulation and Delivery Systems: 40th Volume, Formulation, Application and Adjuvant Innovation*. ASTM International (2020). DOI [10.1520/STP162720190120](https://doi.org/10.1520/STP162720190120). URL https://asmedigitalcollection.asme.org/astm-ebooks/book/chapter-pdf/7216983/10_1520_stp162720190120.pdf, URL <https://doi.org/10.1520/STP162720190120>.
- [12] Khan, Adrees, Nasir, Fazal, Tufail, Muhammad, Haris, Muhammad, Khan, Muhammad Tahir and Dong, Zhang. "Design and Implementation of Model Predictive Control (MPC) Based Pressure Regulation System for a Precision Agricultural Sprayer." *2023 International Conference on Robotics and Automation in Industry (ICRAI)*: pp. 1–6. 2023. DOI [10.1109/ICRAI57502.2023.10089578](https://doi.org/10.1109/ICRAI57502.2023.10089578).
- [13] Nasir, Fazal E, Alam, Muhammad Shahab, Tufail, Muhammad and Khan, Muhammad Tahir. "A Novel Pressure and Flow Control Technique for Variable-Rate Precision Agricultural Sprayer." *2021 International Conference on Robotics and Automation in Industry (ICRAI)*: pp. 1–6. 2021. DOI [10.1109/ICRAI54018.2021.9651446](https://doi.org/10.1109/ICRAI54018.2021.9651446).
- [14] Guo, Yaohua, Liu, Cunjia and Coombes, Matthew. "Spraying Coverage Path Planning for Agriculture Unmanned Aerial Vehicles." *2021 26th International Conference on Automation and Computing (ICAC)*: pp. 1–6. 2021. DOI [10.23919/ICAC50006.2021.9594271](https://doi.org/10.23919/ICAC50006.2021.9594271).
- [15] *Modular and Reconfigurable Multiple Drive-Unit Based Rover - Design and Control*, Vol. Volume 2: Advanced Design and Information Technologies of ASME International Mechanical Engineering Congress and Exposition (2023). DOI [10.1115/IMECE2023-112155](https://doi.org/10.1115/IMECE2023-112155). URL <https://asmedigitalcollection.asme.org/IMECE/proceedings-pdf/IMECE2023/87592/V002T02A002/7238428/v002t02a002-imece2023-112155.pdf>, URL <https://doi.org/10.1115/IMECE2023-112155>.
- [16] LeVoir, Samuel J., Farley, Peter A., Sun, Tao and Xu, Chong. "High-Accuracy Adaptive Low-Cost Location Sensing Subsystems for Autonomous Rover in Precision Agriculture." *IEEE Open Journal of Industry Applications* Vol. 1 (2020): pp. 74–94. DOI [10.1109/OJIA.2020.3015253](https://doi.org/10.1109/OJIA.2020.3015253).
- [17] Bogue, R. "Robots poised to revolutionise agriculture." Vol. 43 No. 5 (2016).
- [18] Hajjaj, S. S. H. and Sahari, K. S. M. "Review of agriculture robotics: Practicality and feasibility." *2016 IEEE International Symposium on Robotics and Intelligent Sensors (IRIS)*: pp. 194–198. 2016. DOI [10.1109/IRIS.2016.8066090](https://doi.org/10.1109/IRIS.2016.8066090).
- [19] Cheein, Fernando Auat, Herrera, Daniel, Gimenez, Javier, Carelli, Ricardo, Torres-Torriti, Miguel, Rosell-Polo, Joan R., Escolà, Alexandre and Arnó, Jaume. "Human-robot interaction in precision agriculture: Sharing the workspace with service units." *2015 IEEE International Conference on Industrial Technology (ICIT)*: pp. 289–295. 2015. DOI [10.1109/ICIT.2015.7125113](https://doi.org/10.1109/ICIT.2015.7125113).
- [20] Vasconez, Juan P., Kantor, George A. and Auat Cheein, Fernando A. "Human-robot interaction in agriculture: A survey and current challenges." *Biosystems Engineering* Vol. 179 (2019): pp. 35 – 48. DOI <https://doi.org/10.1016/j.biosystemseng.2018.12.005>. URL <http://www.sciencedirect.com/science/article/pii/S1537511017309625>.
- [21] WWF. "No Food Left Behind." <https://shorturl.at/YiVVb>. (10 Jun 2024). Accessed: 1 Aug 2024.
- [22] Yandun Narvaez, F., Reina, G., Torres-Torriti, M., Kantor, G. and Cheein, F. A. "A Survey of Ranging and Imaging Techniques for Precision Agriculture Phenotyping." *IEEE/ASME Transactions on Mechatronics* Vol. 22 No. 6 (2017): pp. 2428–2439. DOI [10.1109/TMECH.2017.2760866](https://doi.org/10.1109/TMECH.2017.2760866).
- [23] Spray, One Smart. "One Smart Spray." (One Smart Spray). URL <https://www.onesmartspray.com/>. 2023.
- [24] Deer, John. "See and Spray Technology." <https://shorturl.at/djZu>. (2024). Accessed: 1 May 2024.